A NANO-SCALE FABRY-PEROT INTERFEROMETER USING CHANNEL PLASMON-POLARITONS IN TRIANGULAR METALLIC GROOVES.

D. F. P. Pile[1], D. K. Gramotnev[2]

[1]*Department of Optical Science and Technology, Faculty of Engineering, The University of Tokushima, Minamijosanjima 2-1, Tokushima 770, Japan*

[2]*Applied Optics Program, School of Physical and Chemical Sciences, Queensland University of Technology, GPO Box 2434, Brisbane, QLD 4001, Australia.*

Abstract

In this letter, we demonstrate the possibility of an effective nano-scale Fabry-Perot interferometer in a sub-wavelength plasmonic waveguide in the form of a triangular groove on a metal surface, guiding channel plasmon-polaritons (CPPs). The resonant cavity is formed by two semitransparent metal membranes (mirrors) placed into the groove. Effective filtering effect of the cavity is demonstrated, resulting in single-mode output from the cavity. Typical quality factor for the cavity of the resonant length is determined to be Q ~ 100 for the silver-vacuum structure with the 30^o groove angle. Possible ways of increasing this factor are discussed.

A major current problem in modern photonics is the diffraction limit of light [1-3] that does not allow localization of electromagnetic waves in regions noticeably smaller than half the wavelength in the structure. This results in a much lower level of integration and miniaturization of optical devices, compared to that achieved in modern microelectronics. A main direction to overcome this diffraction limit and achieving sub-wavelength localization is related to use of plasma waves (plasmons) in metallic nano-sized structures. These include metallic nano-strips [4-9], nano-rods [2,10], nano-chains [1,3,11,12], metal slits [13], etc. However, major problems with these structures include excessive dissipation [1,3,7,9], expected significant losses at sharp bends [12], high sensitivity to structural imperfections, etc. Therefore, a new type of strongly localized plasmons – channel plasmon-polaritons (CPPs) – has recently been analyzed in metallic grooves [14-16]. CPPs in V-grooves have demonstrated superior features from the view-point of sub-wavelength guiding, including a unique combination of strong localization and relatively low dissipation [15,16], single-mode operation [16], and a possibility of nearly 100% transmission through sharp bends [17].

The aim of this letter is to demonstrate a possibility of design of efficient nano-optical devices, such as a Fabry-Perot interferometer and nano-sized cavity, using CPPs in triangular groove waveguides. Main features of such an interferometer/cavity will be analyzed numerically, using the finite-difference time-domain (FDTD) algorithm.

The analyzed structure is presented in Fig. 1a. Two semitransparent metallic membranes (mirrors) of the same thickness l_m are inserted perpendicular to the triangular groove on a silver surface, so that the distance between these membranes is L (Fig. 1a).

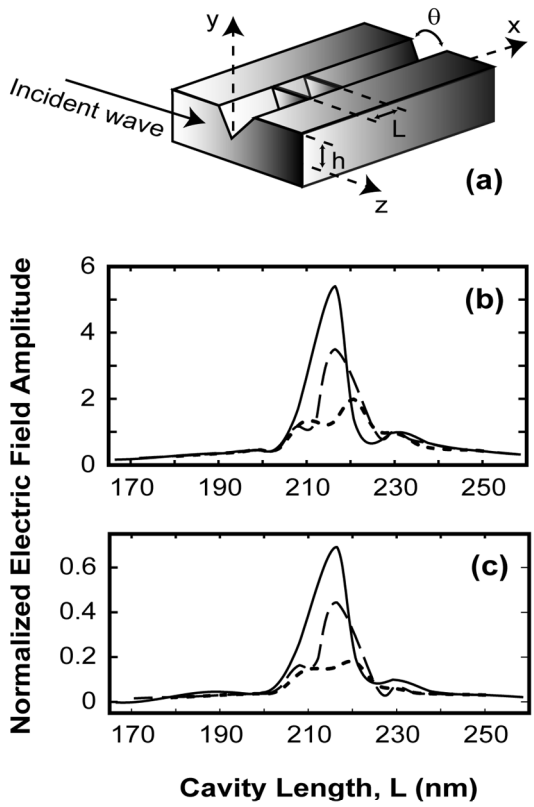

Fig. 1. (a) The structures with a V-groove sub-wavelength waveguide with two metallic membranes (mirrors) forming a Fabry-Perot interferometer of length L. CPP modes are generated by the end-fire excitation using a bulk plane wave incident at the angle of 45^o to the x-axis. The incident wave is generated by the z-component of the magnetic field. (b,c) The dependencies of the amplitudes of the electric field: (b) in the middle of the cavity, and (c) in the wave transmitted through the cavity on cavity length L for the silver-vacuum structure at the vacuum wavelength $\lambda_{vac} = 0.6328$ μm in the absence of dissipation (the dielectric permittivity of the metal is real: $\varepsilon_m = -16.22$) at three different moments of time $t_1 = 1.22\times10^{-13}$ s (dotted curves), $t_2 = 2.44\times10^{-13}$ s (dashed curves), and $t_3 = 4.88\times10^{-13}$ s (solid curves). The thickness of the cavity mirrors $l_m = 42.2$ nm, $\theta = 30^o$. The electric field amplitudes are normalized to the amplitude of the incident wave at the point of consideration in the absence of the cavity.

The analysis is carried out by means of the FDTD algorithm that was previously developed and used in [15-17] for the investigation of CPP modes in straight V-grooves and sharp bends. CPP modes are generated in the silver-vacuum groove with the cavity

(Fig. 1a). The dielectric permittivity of silver is determined using the local Drude model for the incident wavelength in vacuum $\lambda_{vac} = 0.6328$ μm (He-Ne laser). The free electron charge density $\rho \approx -7.684\times10^{9}$ C/m^3 and damping frequency $f_d \approx 1.4332\times10^{13}$ Hz [18,19] (corresponding to dielectric permittivity of silver $\varepsilon_m \approx -16.22 + 0.52i$). The mirrors of the cavity are also made of silver with the same ε_m.

The depth of the groove $h \approx 1.6$ μm is determined by the size of the computational window, which is significantly larger than the penetration depth of the fundamental CPP up the sides of the groove (~ 170 nm [15,16]). Therefore, the results will effectively correspond to an infinitely deep groove.

The size of the FDTD grid cells outside of the cavity is $\lambda_{vac}/30$ (i.e., ≈ 21.1 nm) along the *x*-axis (Fig. 1a). However, this is insufficient for optimization of the thickness of the mirrors and cavity length. Therefore, a non-uniform grid has been used with the grid cells along the *x*-axis inside the cavity and the membranes (mirrors) being $\lambda_{vac}/300$ and $\lambda_{vac}/150$, respectively. Along the *y*-axis and *z*-axis, the grid spacing is $\lambda_{vac}/60$ everywhere in the computational window.

Figs. 1b,c present the numerical dependencies of the normalized amplitudes of the electric field in the middle of the cavity (Fig. 1b), and in the wave transmitted through the cavity (Fig. 1c) at zero dissipation in the metal ($f_d = 0$) at three different moments of time after switching the incident wave on at $t = 0$. It can clearly be seen that the amplitudes of the field in the cavity and behind it resonantly increase in time at the cavity length $L \approx 216.5$ nm. The solid curves approximately correspond to the steady-state case, whereas the dashed and dotted curves correspond to strongly non-steady-state regimes. The resonant behavior of the field inside and behind the cavity clearly demonstrates that the considered simple arrangement with just two membranes (mirrors) across the groove can indeed work as a Fabry-Perot resonator/interferometer. Further

increase of the thickness of the mirrors of the interferometer results in a rapid increase of the height and sharpness of the observed resonance. In particular, this suggests that there is no significant leakage of the energy from the cavity (away from the tip of the groove) in the form of surface and/or bulk waves. At the same time, numerical analysis using FDTD algorithm at mirror thicknesses l_m that are noticeably larger than ~ 42.2 nm is difficult due to exponentially increasing relaxation (and computational) time and the corresponding accumulation of numerical errors.

It is reasonable to expect that dissipation in the metal should have a significant effect on the presented dependencies (Fig. 1b,c). Indeed, if we assume that the dielectric permittivity of silver is $\varepsilon_m = -16.22 + 0.52i$, then the corresponding L-dependencies of the amplitudes of the electric field in the cavity and behind it are shown in Figs. 2a,b.

One of the main aspects is that the resonance in Figs 2a,b has significantly dropped in height compared to the case without dissipation (Fig. 1b). If the mirror thickness is increased, then the leakage from the cavity through the mirrors is reduced, but the effect of dissipation in the metal inside the cavity is increased (due to increased relaxation time). As a result, the resonance becomes lower and broader (curves 1 in Fig. 2). On the other hand, if the thickness of the mirrors is decreased, the effect of dissipation inside the cavity is reduced, due to decreased relaxation time, but the leakage through the mirrors is increased. As a result, the resonance also becomes weaker and broader (curves 3, 4 in Fig. 2). Therefore, there exists an optimal membrane thickness ($l_{mo} \approx 42.2$ nm) at which the resonance is strongest and sharpest (curves 2 in Fig. 2). At this optimal membrane thickness, the full width half maximum (FWHM) of the resonance curve is ~ 10 nm, which corresponds to the quality factor of the cavity Q ~ 100.

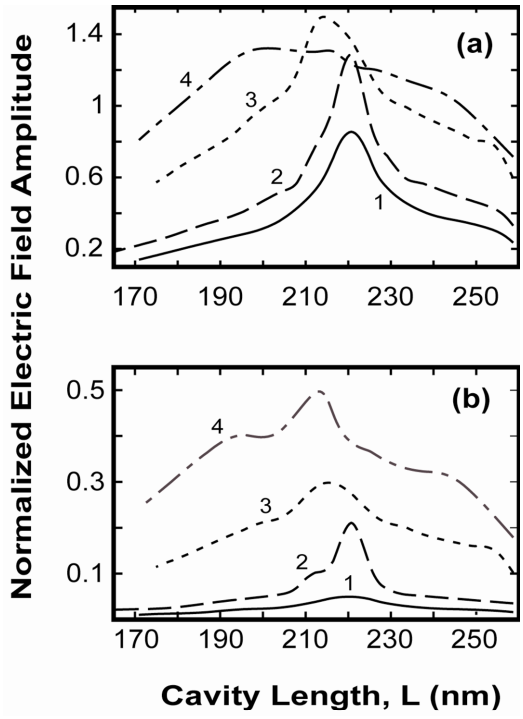

Fig. 2. The steady-state dependencies of the amplitudes of the electric field: (a) in the middle of the cavity and (b) in the wave transmitted through the cavity on cavity length L in the presence of dissipation ($\varepsilon_m = -16.22 + 0.52i$) at different thicknesses of the cavity mirrors: (1) $l_m = 50.6$ nm, (2) $l_m = 42.2$ nm, (3) $l_m = 25.3$ nm, (4) $l_m = 16.9$ nm. $\theta = 30^o$, $\lambda_{vac} = 0.6328$ μm. The electric field amplitudes are normalized to the amplitude of the incident wave at the point of consideration in the absence of the cavity (membranes).

Possible ways of increasing Q are related to reducing the effect of dissipation on the CPP mode. This could be achieved by using gain-assisted CPP modes, similar to gain-assisted surface plasmons [20]. In this case, the groove and the cavity can be filled by a medium with gain, which will cancel or reduce the effect of dissipation, significantly increasing the sharpness and strength of the resonance (Figs. 1b,c).

Fig. 3a presents the time evolution of the field amplitudes in front of, inside, and behind the cavity for two different cavity lengths: $L = 220.7$ nm and 170.1 nm. The first

value of L corresponds to the resonance in the cavity at l_m = 42.2 nm (Fig. 2), while the second is sufficiently far from the resonant value.

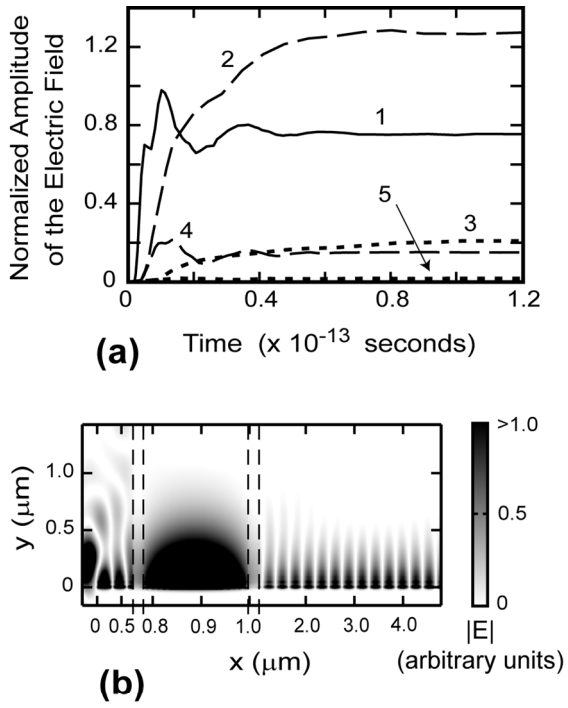

Fig. 3. (a) The time dependencies of the normalized amplitude of the electric field in front of the cavity (solid curve), in the middle of the cavity (dashed curves), and behind the cavity (dotted curves) at two different cavity lengths: $L = L_r \approx 220.7$ nm (curves 1 – 3), and (b) L = 170.1 nm (curves 1, 4, 5). l_m = 42.2 nm, and the other structural parameters are the same as for Fig. 2. (b) The distribution of the magnitude of the electric field in the (x,y) plane inside the groove, cavity and the mirrors at the resonant cavity length L = 220.7 nm and l_m = 42.2 nm. The scale along the x-axis in the mirrors and the cavity is 5 and 10 times larger than outside of the cavity. These regions are indicated by four dashed vertical lines. The end-fire excitation occurs at x = 0.

It can be seen that if the cavity length is not equal to the resonant length, the transmitted wave in next to zero (curve 5 in Fig. 3a), which demonstrates the filtering effect of the cavity. The amplitude of the field in front of the cavity is practically the same (with the difference of less than ~ 3%) for both the cavity lengths. Therefore, this amplitude is given by just one curve 1 (Fig. 3a). It goes through a maximum (that is

equal to one), and then decreases with oscillations to ≈ 0.79. This is because the incident CPP modes experience multiple reflections from the front mirror and the end of the groove where end-fire excitation occurs. At the considered length of the groove in front of the cavity (≈ 1.08 μm), the wave reflected from the end of the groove appears to be in destructive interference with the CPP mode generated directly by the end-fire excitation. This results in a reduction of the overall steady-state incident wave amplitude in front of the cavity (curve 1 in Fig. 3a). Different length of the initial section of the groove will result in different values of the overall amplitude of the incident CPP mode (smaller or larger than one). Thus position of the cavity in the groove is also important for the design of nano-optics interferometers and filters.

The field distribution in the (x,y) plane in the groove and the cavity is presented in Fig. 3b. The scale along the x-axis in the cavity and membranes (mirrors) is magnified 10 and 5 times, respectively, in accordance with the finer non-uniform grid inside these regions (see above).

Two important aspects can be determined from Fig. 3b. Firstly, as shown in [15], end-fire excitation in the considered structure results in generation of two different CPP modes in the groove, causing strong beats in the field structure along the groove. Therefore, both the modes are generated in Fig. 3b in front of the cavity. Nevertheless, only one fundamental mode is effectively transmitted through the cavity of the resonant length L = 220.7 nm (this is confirmed by Fourier analysis of the output). Therefore, this is a clear demonstration that the cavity works as a filter for CPP modes, resulting in single-mode output (Fig. 3b).

Secondly, as can be seen from the presented field distribution (Fig. 3b), hardly any leakage can be seen from the cavity in the form of bulk and/or surface waves up the walls of the cavity (see also discussion of Figs. 1b,c). Thus, vertical membranes inserted

into the groove do not result in an uncontrollable scattering of the guided CPP mode. Physical explanation for this effect is mainly related to the sub-wavelength localization of the fundamental CPP mode in the considered structure (within the region of ~ 120 – 170 nm [15,16]). The field is significant only in the region where the width of the groove (~ 100 nm) is still much less than the wavelength of a bulk wave (632.8 nm). As a result, generation of bulk waves in such a narrow sub-wavelength gap is strongly impeded. On the other hand, in the region where the groove is sufficiently wide for a bulk wave to propagate, the field due to the CPP mode is negligible. Therefore, leakage from the cavity in the form of scattered bulk and surface waves is negligible (Fig. 3b).

Note however, that if the angle of the groove is increased, the leakage due to scattered bulk and surface waves at the mirrors of the cavity may increase. This is because increasing groove angle results in decreasing CPP localization [15], and the region in which the field is significant may extend well into the region where bulk waves can easily be generated. As a result, efficient scattering into bulk and surface waves becomes possible in this case.

In conclusion, we have demonstrated that a nano-scale Fabry-Perot interferometer (cavity) can be designed using CPP modes in a triangular groove on a metal substrate. Typical values of the quality factor that can be achieved in the silver-vacuum grooves are about 100. However, use of gain-assisted CPP modes may result in a significant increase of this factor and typical propagation distances of CPP modes. A possibility of effective filtering of optical signals in the considered sub-wavelength waveguide with a nano-sized cavity has also been demonstrated.

The authors gratefully acknowledge support from the Japan Society for the Promotion of Science and the High Performance Computing Division at the Queensland University of Technology.

References

1. J. R. Krenn, *Nature Mater* **2,** 210 (2003).
2. J. Takahara, S. Yamagishi, H. Taki, A. Morimoto, T. Kobayashi, *Opt. Lett*. **22**, 475 (1997).
3. S. A. Maier, P. G. Kik, H. A. Atwater, S. Meltzer, E. Harel, B. E. Koel, A. A. G. Requicha, *Nature Mater*. **2**, 229 (2003).
4. R. Charbonneau, P. Berini, E. Berolo, E. Lisicka-Shrzek, *Opt. Lett*. **25**, 844 (2000).
5. P. Berini, *Phys. Rev*. **B61**, 10484 (2000); *Phys Rev.* **B63**, 125417 (2001).
6. T. Nikolajsen, K. Leosson, I. Salakhutdinov, S. Bozhevolnyi, *Appl. Phys. Lett.* **82**, 668 (2003).
7. B. Lamprecht, J. R. Krenn, G. Schider, H. Ditlbacher, M. Salerno, N. Felidj, A. Leitner, F. R. Aussenegg, *Appl. Phys. Lett.* **79**, 51 (2001).
8. G. Schider, J. R. Krenn, A. Hohenau, H. Ditlbacher, A. Leitner, F. R. Aussenegg, W. L. Schaich, I. Puscasu, B. Monacelli, G. Boreman, *Phys. Rev.* **B68**, 155427 (2003).
9. J. R. Krenn, B. Lamprecht, H. Ditlbacher, G. Schider, M. Salerno, A. Leitner, F. R. Aussenegg, *Europhys. Lett*. **60**, 663 (2002).
10. T. Onuki, Y. Watanabe, K. Nishio, T. Tsuchiya, T. Tani, T. Tokizaki, *J. Microscopy* **210**, 284 (2003).
11. J. R. Krenn, A. Dereux, J. C. Weeber, E. Bourillot, Y. Lacroute, J. P. Goudonnet, G. Schider, W. Gotschy, A. Leitner, F. R. Aussenegg, C. Girard, *Phys. Rev. Lett*. **82**, 2590 (1999).
12. S. A. Maier, M. L. Brongersma, H. A. Atwater, *Appl. Phys. Lett.* **78**, 16 (2001).
13. K. Tanaka, M. Tanaka, *Appl. Phys. Lett*. **82**, 1158 (2003).
14. I. V. Novikov, A. A. Maradudin, Phys. Rev. **B66**, 035403 (2002).
15. D. F. P. Pile, D. K. Gramotnev, *Opt. Lett.* **29**, 1069 (2004).

16. D. K. Gramotnev, D. F. P. Pile, Single-mode sub-wavelength waveguide with channel plasmon-polaritons in triangular grooves on a metal surface, *Appl. Phys. Lett.* **85**, 6323 (2004).
17. D. F. P. Pile, D. K. Gramotnev, New plasmonic sub-wavelength waveguides: next to zero losses at sharp bends, *Opt. Lett.* (submitted).
18. D. Christensen, D. Fowers, *Biosens. Bioelectron.* **11**, 677 (1996).
19. Fowers, D., Masters Thesis, University of Utah (1994).
20. M.P. Nazhad, K. Tetz, Y. Fainman, Optics Express, **4072** (2004).